NUCLEATION OF THE WIDMANSTATTEN PATTERN IN IRON METEORITES. J. Yang[1] and J. I. Goldstein[1], [1]Dept. of Mechanical and Industrial Engineering, College of Engineering, University of Massachusetts, Amherst, MA 01003, USA. Email: jiyang@ecs.umass.edu and jig0@ecs.umass.edu.

Introduction: The Widmanstatten pattern develops at low temperatures during the evolution of the asteroids. We have studied the origin of the Widmanstatten pattern in order to obtain metallographic cooling rates in the temperature range (~ 700 to 300 deg C). This paper summarizes our recent evaluation of the various mechanisms for the formation of the Widmanstatten pattern. All chemical groups of the iron meteorites are considered [1, 2]. We also propose a new mechanism for the formation of the Widmanstatten pattern in the low P metal phase of iron, stony-iron and stony meteorites. The results of this evaluation enables us to more accurately determine metallographic cooling rates particularly when incorporated with other recent advances in Fe-Ni and Fe-Ni (P saturated) phase diagrams and interdiffusion coefficients.

Origin of the Widmanstatten Pattern in Meteorites: The formation of the Widmanstatten pattern depends on the bulk Ni and bulk P in a given meteorite. Five mechanisms have been proposed: (i) $\gamma \rightarrow \alpha+\gamma$ (mechanism I): This is the traditional mechanism which is based on the binary Fe-Ni phase diagram. This mechanism assumes that α can nucleate directly from γ phase within the $\alpha+\gamma$ two phase region when cooling from high temperature to low temperature. However, several experimental studies have shown that it is not possible to nucleate α phase directly within single crystal taenite, γ phase, in synthetic Fe-Ni alloys during cooling and before forming martensite, α_2 phase [3, 4]. (ii) $\gamma \rightarrow \gamma+$Ph (phosphide, $(FeNi)_3P) \rightarrow \alpha+\gamma+$Ph (mechanism II): The important role of P in the formation of the Widmanstatten pattern in iron meteorites has been recognized, Goldstein et al. [5]. These authors showed, experimentally, that this mechanism can produce a Widmanstatten pattern in high P containing Fe-Ni-P alloys. (iii) $\gamma \rightarrow \alpha+\gamma \rightarrow \alpha+\gamma+$Ph (mechanism III): This mechanism was proposed by Moren et al. [6] in their cooling rate simulation of low P iron meteorites. However, under-cooling of 120-190 ^{o}C below the equilibrium $\gamma/(\alpha+\gamma)$ phase boundary is necessary in many low P IVA iron meteorites. Narayan et al. [4] investigated, experimentally, the nucleation of intragranular α phase from γ phase in Fe-Ni-P alloys. They found that, in low P Fe-Ni alloys, α phase cannot nucleate when the alloy is cooled into the two-phase $\alpha+\gamma$ field. In fact, the α phase only nucleates when γ phase is saturated in P and enters the $\alpha+\gamma+$Ph field. (iv) $\gamma \rightarrow \alpha_2 \rightarrow \alpha+\gamma$ (mechanism IV): This mechanism was initially proposed as an alternate to mechanism I, $\gamma \rightarrow \alpha+\gamma$, for iron meteorites by Owen [7] and Buchwald [8]. Recently mechanism IV was used to determine the cooling rate of mesosiderites and low P IVA iron meteorites [9, 10]. However, the Widmanstatten pattern cannot form by this mechanism in low P meteorites [2], even though this mechanism is applicable to the formation of the plessite structure in taenite lamellae. (v) ($\gamma \rightarrow \alpha_2+\gamma \rightarrow \alpha+\gamma+$(Ph)) (mechanism V): This mechanism was recently proposed by Yang et al. [1, 2] and can be used to explain the origin of the Widmanstatten pattern in low P meteorites. In this case, α_2 forms once the martensite start temperature is crossed during cooling and before P saturation occurs. The kamacite phase nucleates near the M_s temperature by the reaction $\alpha_2 \rightarrow \alpha+\gamma$.

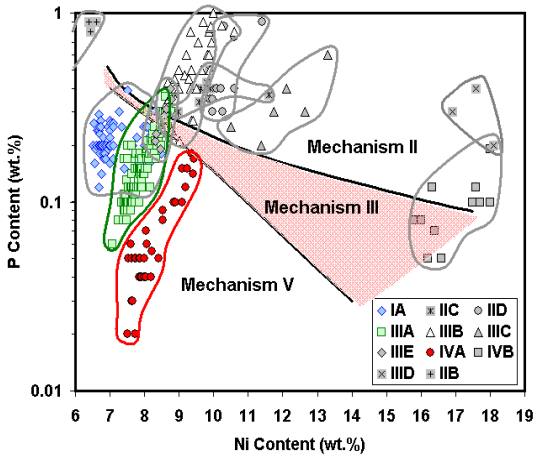

Fig. 1. Regions of three mechanisms (II, III and V) for the formation of the Widmanstatten pattern and bulk Ni and P contents in eleven iron meteorites.

Of the five mechanisms (I-V) summarized above, three mechanisms (II, III and V) are applicable to the formation of the Widmanstatten pattern. The applicability of each mechanism depends on the bulk Ni and bulk P in metal phase of meteorites. Fig. 1 shows the applicable Ni-P regions for the three mechanisms. The bulk Ni and bulk P of eleven iron meteorite groups, Buchwald [11], are also plotted in this figure. The Widmanstatten pattern formed by mechanism II ($\gamma \rightarrow \gamma+$Ph (phosphide, $(FeNi)_3P) \rightarrow \alpha+\gamma+$Ph) in most of the group members in IIC, IID, IIIB, IIIC and IIID, and by mechanism V ($\gamma \rightarrow \alpha_2+\gamma \rightarrow \alpha+\gamma+$(Ph)) in groups IA, IIIA and IVA. The origin of the Widmanstatten

pattern in stony-iron meteorites and a few chondrites can also be determined explicitly through Fig.1 based on their bulk Ni and bulk P contents.

Metallographic Cooling Rates of Meteorites: For a given meteorite containing the Widmanstatten pattern, the determination of the cooling rate depends on three factors: formation mechanism of the Widmanstatten pattern (discussed previously), Fe-Ni and Fe-Ni-P phase diagrams, and interdiffusion coefficients. Fig. 2 shows an example of a cooling rate simulation using the central taenite Ni method for the Widmanstatten pattern [1, 2] in a IVA iron, Duchesne, the Fe-Ni phase diagram [12] and Fe-Ni (P saturated) phase diagram [13], and the applicable Fe-Ni (P) interdiffusion coefficients [14]. The calculated cooling rate based on mechanism V matches the measured data (Fig.2). However, the calculated cooling rate based mechanism II can only match part of the measured data.

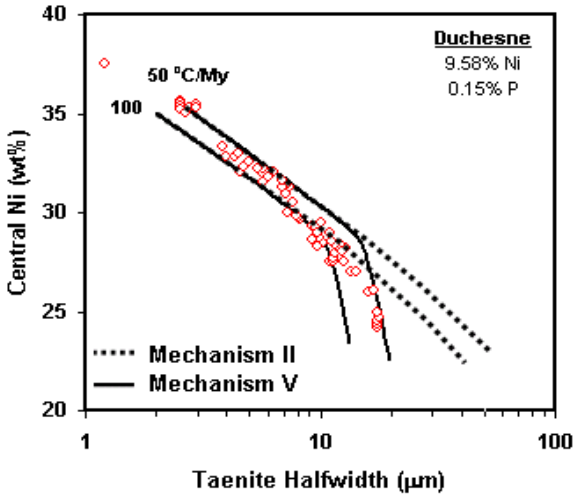

Fig. 2. Cooling rate curves based on two different mechanisms for the formation of the Widmanstatten pattern in Duchesne iron meteorite (IVA). Experimental data (circle dot) are from Moren et al. [6].

Implications of this study to the Determination and Explanation of Cooling Rates: First, using Fig. 2, we observe that the determination of the cooling rate depends strongly on the correct choice of the nucleation mechanism of the Widmanstatten pattern. For example, the origin of the Widmanstatten pattern in high P meteorites can not be used in low P meteorites.

Second, we observe (Fig. 2) that the cooling rates of a given meteorite should be obtained by comparing the calculated and measured data both from narrow and wide taenite lamellae.

Third, it is possible that the same cooling rate can be obtained by different nucleation mechanisms such as mechanism II and mechanism V. For example, narrow taenite lamellae data (<10μm in Fig.2) give the same cooling rates for Mechanisms II and V. Even though the cooling rates are the same, the cooling rate obtained using mechanism II relates to a higher temperature than that obtained by mechanism V. For Duchesne, the difference in the kamacite nucleation temperatures based on these two mechanisms (II vs V) is at least 100 ^{o}C.

Finally, when calculating the cooling rates for multiple meteorites within a chemical group, obtaining the same cooling rates may not mean that these rates are for the same temperature range. Therefore, special care must be taken when cooling rates are used to infer the structure of meteorite parent bodies.

Acknowledgements: The authors would like to thank the financial support from NASA through grant NAG5-11778.

References: [1] Yang J. and Goldstein J. I. (2003) MAPS, 38, A33. [2] Yang J. and Goldstein J. I. (2003) MAPS, in review. [3] Allen N. P. and Earley, C. C. (1950) JISI, 166, 281-88. [4] Narayan C. and Goldstein J. I. (1984). Metall. Trans., 15A, 861-65. [5] Goldstein J. I. and Doan A. S. (1972) Geochim. Cosmochim. Acta, 36, 51-69. [6] Moren A. E. and Goldstein J. I. (1979) EPSL, 43, 182-96. [7] Owen E. A. (1940) Philosophical magazine, 29, 553-67. [8] Buchwald V. F. (1966) Acta Polytechnica Scandinavica, 51, 1-45. [9] Hopfe W. D. and Goldstein J. I. (2000) MAPS, 35, A77. [10] Goldstein J. I. and Hopfe W. D. (2001) MAPS, 36, A67. [11] Buchwald V. F. (1975) Handbook of Iron Meteorites. Their History, Distribution, Composition and Structure. Berkeley and Los Angeles, CA, University of California Press, 1-1418. [12] Yang C.-W. et al. (1996) J. Phase Equilibria, 17, 522-31. [13] Yang J. and Goldstein J. I. (2003) unpublished. [14] Yang J. and Goldstein J. I. (2004) Metall. & Mats. Trans., in press.